JOURNAL OF MATERIALS SCIENCE **36** (2001) 1293–1300

Mechanical properties of SG-iron with different matrix structure

M. HAFIZ
Al-Azhar University, Faculty of Engineering, Department of Mechanical Engineering, Nasr City, Cairo, Egypt
E-mail: mfhafiz@frcu.eun.eg

Spheroidal graphite (SG) irons with a variety of matrix-structure have been produced. The correlation between tensile properties, impact toughness, hardness and pearlite content is investigated. The pearlite content is varied from 0 to about 95 per cent by the use of different heat treatment processes. The apparent variation in the properties with the pearlite level reveals the remarkable consistency in the relationships between mechanical properties and pearlite content. The study of the tensile properties showed that the yield and ultimate tensile strengths are increased with increasing pearlite level in the matrix structure. For matrix structure with 94.6% pearlite, the increases are about 91% and 98%, respectively, compared with those of the ferritic matrix material. The impact toughness of SG-iron is influenced significantly by matrix microstructure. Energy of about 230×10^3 J/m^2 is required to fracture a ferritic matrix SG-iron. On the other hand, when the matrix structure approaches a fully pearlitic matrix the fracture energy is decreased by an amount of 75.5%. The Brinell hardness value is found to increase with increasing pearlite content in the matrix structure of the present material. It increases from about 128 for a fully ferritic matrix to about 258 as the matrix structure approaches a fully pearlitic condition. This change in the hardness value reflects the change in the mechanical properties presented in this study.

1. Introduction

Spheroidal graphite (SG) irons are very unique engineering materials, possessing good castability and mechanical properties. The feature that all the members of SG-irons share is the roughly spherical shape of the graphite nodules. However, with a high percentage of graphite nodules present in the structure, the control of the SG-iron matrix structure is of potential importance. A number of variables including chemical composition, cooling rate, type, amount and method of post inoculation, amount of residual magnesium and pouring temperature can control the matrix structure of SG-iron [1–7]. Heat treating of SG-iron is also another rout to produce a family of materials offering a wide range of properties obtained through matrix microstructure control [8–10]. The importance of matrix in controlling mechanical properties is emphasized by the use of matrix names to designate the types of SG-iron [11, 12].

Graphite spheroids in a matrix of ferrite provide an iron with good ductility and impact resistance and with a tensile and yield strength equivalent to low carbon steel. In a matrix containing both ferrite and pearlite properties intermediate between ferritic and pearlitic grades is obtained, with good machinability and low production costs. A pearlitic matrix results in an iron with high strength, good wear resistance, and moderate ductility and impact resistance. In this material machinability is also superior to steel of comparable physical properties. Using sufficient alloy additions to prevent pearlite formation and a quench-and-temper heat treatment produces a martensitic SG -iron. The resulting tempered martensite matrix develops very high strength and wear resistance but with lower levels of ductility and toughness. Bainitic SG-iron can be obtained through alloying and/or by heat treatment to produce a hard, wear resistant material. Austenitic matrix SG-iron offers good corrosion and oxidation resistance, good magnetic properties, and good properties at elevated temperatures. Austempered ductile iron (ADI), the most recent addition to the SG-iron family, is a subgroup of SG-iron produced by giving conventional SG-iron a special austempering heat treatment after which the iron still retains high elongation and toughness. This heat treatment also results in a material with superior wear resistance and fatigue strength.

To summarize, SG-iron is a prime example of materials where the properties achieved depend upon the characteristics of the microstructure. This microstructure is determined in part during solidification (graphite shape, size and distribution) and in part during solid-state transformation (matrix). It is the development of the matrix structure that is of concern in this study. The influence of the matrix structure on the mechanical properties and impact toughness is investigated.

TABLE I Chemical composition of SG-iron

Element	C	Si	S	P	Mn	Ni	Cr	Mo	Mg	Fe	CE*
Mass%	3.6	2.29	0.011	0.053	0.08	0.022	0.025	0.007	0.055	Bal.	4.381

*CE = C + 1/3 (Si + P).

2. Experimental procedure

The charge used to produce SG-iron consisted of pig iron, return SG-iron and steel scrap. Melting is performed in an induction furnace with a melting capacity of 6 tons. Spheroidization treatment has been carried out using the ladle transfer method. In this method, a magnesium master alloy containing 45Fe-50Si-5Mg is placed in the bottom of the treatment ladle and the molten metal is poured over it. To prevent Mg evaporation and/or burning, the master alloy has been covered with pieces of steel or some other material before liquid iron is poured into the ladle. This is called a sandwich technique. The melt is postinoculated using 75% ferrosilicon alloy, prior to pouring. The chemical analysis of the SG-iron used in the present work is carried out using spectrometer. Table I displays the composition of the present alloy.

Five ingots are produced by pouring the molten metal at ~1598 K into Y-shaped sand moulds. The dimensions of each Y-block are 40 × 80 × 210 mm, in the parallel portion. Fig. 1 shows the cast ingot together with its dimensions. After pouring the cast ingots are left to cool, in the mould, to room temperature (~300 K).

In the present work, the cast ingots are divided into five groups. The material in the first group is used directly in the experiments without any additional heat treatment (i.e. as-cast). For the second group the material is subjected to ferritic heat treatment. The ferritization procedure followed the usual two stage isothermal holding, in which SG-iron is held at 1193 K for 18 ks, furnace cooled to 993 K for the second isothermal holding for 25.2 ks, and then furnace cooled to room temperature (~300 K). Fig. 2a shows the ferritic heat treatment used in the present study. The materials of the remaining groups are heated to 1193 K, held for 18 ks at this temperature, then cooled to room temperature following different cooling rates, namely still air cooled, forced air cooled and cooled in an isolated block in still air, as shown schematically in Fig. 2b.

To reveal the effect of different heat treatment processes on the matrix microstructure, optical microscopy is performed on polished and etched specimens. These

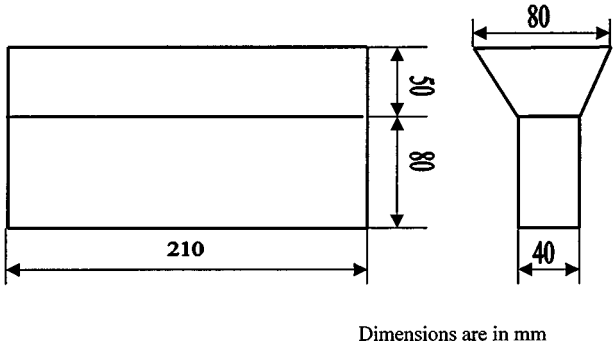

Figure 1 Shows Y-block ingot.

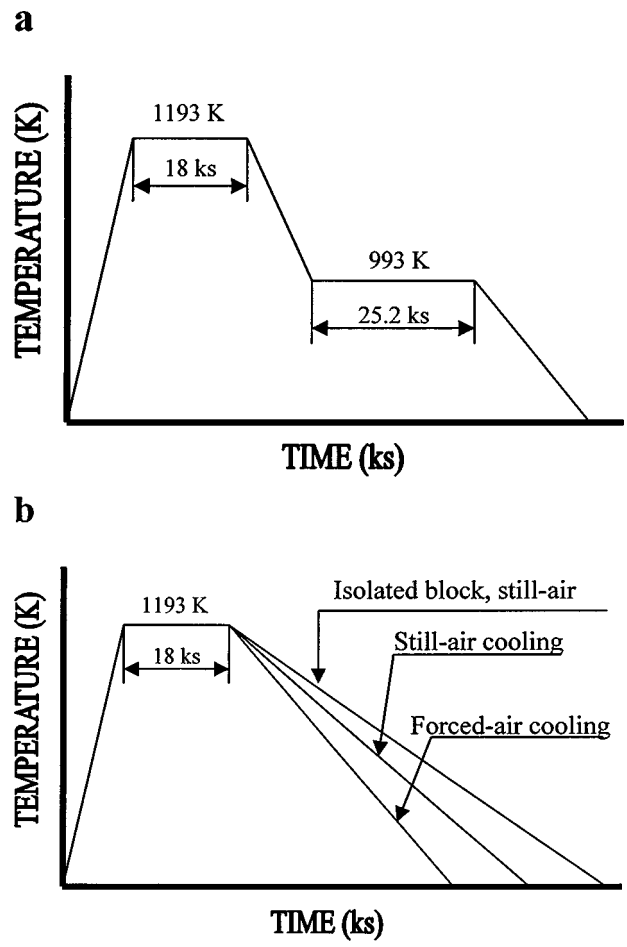

Figure 2 Heat treatment cycles used in the present study: (a) Ferritic heat treatment; (b) Pearlitic heat treatment.

specimens are prepared using standard metallographic technique [13] and are examined after etching with 4% nital. To eliminate the possibility of linking the results with unrepresentative microstructure, metallographic specimens are taken directly from the tested material. The volume fraction of the different phases has been determined using point counting technique [14]. The volume fraction measurements are carried out on micrographs with magnifications of 80 and 160, depending on the fineness of the constituent phases.

A static tension test has been carried out using standard round test specimens with a gauge diameter of 5 mm and a gauge length of 25 mm. The test is conducted in a motor driven tensometer machine "type - W", at a constant cross head speed of about 0.02 mm/s, at room temperature (300 K). The load-extension curve is recorded till fracture. Then, the tensile properties (0.2% proof stress, ultimate tensile strength and elongation %) are determined.

The effect of the matrix structure on the impact toughness has been investigated. The fracture energy (Et) is used as a measure of the toughness of SG-irons

under consideration. The tests are conducted on standard Charpy, 10 × 10 × 55 mm; V-notch specimens.

Brinell Hardness is frequently used for production control and as an auxiliary property test, for example to control machinability. Thus, in the present work this type of hardness tests is carried out.

3. Results and discussions

3.1. Microstructure

Fig. 3 shows the microstructure of the present material after ferritic heat treatment. Spheroidal graphite embedded in a fully ferritic matrix, with no traces of pearlite phase, can be seen. When the matrix structure of SG-iron shows a pearlite content ranging from 10 to 60%, it can be rated as ferritic-pearlitic SG-iron [15]. Fig. 4a, b is an example of ferritic-pearlitic SG-irons. The photo shown in Fig. 4a represents the microstructure of the present material in the as-cast condition while that of Fig. 4b depicts the microstructure after austenitization at 1193 K for 18 ks and cooling in isolation of direct air. The microstructure shown in Fig. 4 is typical "bull's-eye" structure in which many of the graphite nodules are surrounded by an envelope of ferrite. Both the graphite nodules and their ferrite envelopes are embedded in a pearlitic matrix. There is also some free ferrite, which is not associated with graphite. It is worthy to note that the volume fraction of the pearlite phase (P%) in the former is less than that of the latter, (cf. Table II). When austenitized at 1193 K for 18 ks and then cooled in still air or forced air, the matrix structure is essentially pearlite, although ferrite halos are developed around the graphite nodules, Fig. 5a, b. As can be seen, the pearlite content of the latter is about 94.6% while that of the former is about 75.6% (cf. Table II). In other words, the pearlite to ferrite ratio (P/F) has been increased from about 3.1 in the still air-cooled ingot to 19 for the forced air-cooled one. This is because the faster cooling rate of the latter. It is also noted that there is a ferrite imbedded in pearlite. This ferrite formed without any particular relation to the graphite nodules (cf. Fig. 5a).

The most significant difference between the microstructures shown in Figs 4 and 5 is that a complete thick ferrite ring in the as-cast and isolated conditions (Fig. 4) generally surrounds graphite nodules. In still-air cooled structure this ferrite ring is thinner (Fig. 5a), while the forced-air cooled material the ferrite area distributed near the nodules in a discontinuous way (Fig. 5b). Thus, a number of triple points (ferrite-pearlite-graphite) are present in the later material.

TABLE II Volume fraction of pearlite phase in the matrix structure of SG-iron used in the present study

Condition	Pearlite level (%)
Ferritic heat treatment	00.0
Austenitized at 1193 K for 18 ks then cooled in isolated block, in still-air	41.6
As-cast	58.5
Austenitized at 1193 K for 18 ks followed by cooling in still-air	75.6
Austenitized at 1193 K for 18 ks followed by forced-air cooling	94.6

3.2. Tensile properties

Fig. 6 shows the correlation between tensile properties and pearlite content. The pearlite content is varied from 0%, (in fully ferritic structure) to 94.6% (in fully pearlitic structure), by the use of different heat treatment cycles. The apparent variation in tensile properties is an indication of the effects of matrix structure. It can be seen that, the tensile properties vary mainly through the influence of the pearlite content of the matrix. 0.2% yield and ultimate tensile strengths increase, and elongation decreases, until the matrix becomes fully pearlitic. As can be seen, the 0.2% yield strength ranges from 240 MPa for ferritic to 457 MPa for pearlitic matrix SG-iron. The ultimate tensile strength (UTS) of the present material is also increased due to the increase of pearlite level, Fig. 6b. Compared to the fully ferritic matrix material, the percentage increase of the UTS is found to be about 25% in a ferritic/pearlitic matrix. The percentage increase of this property is about 94% for

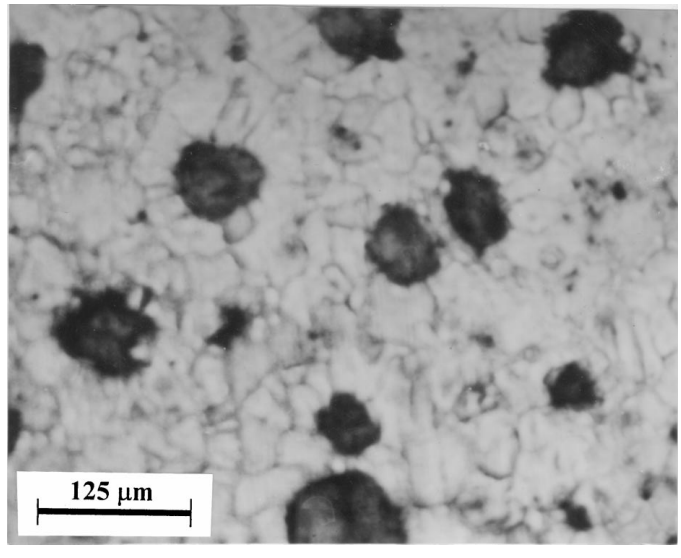

Figure 3 Microstructure of ferritic matrix SG-iron.

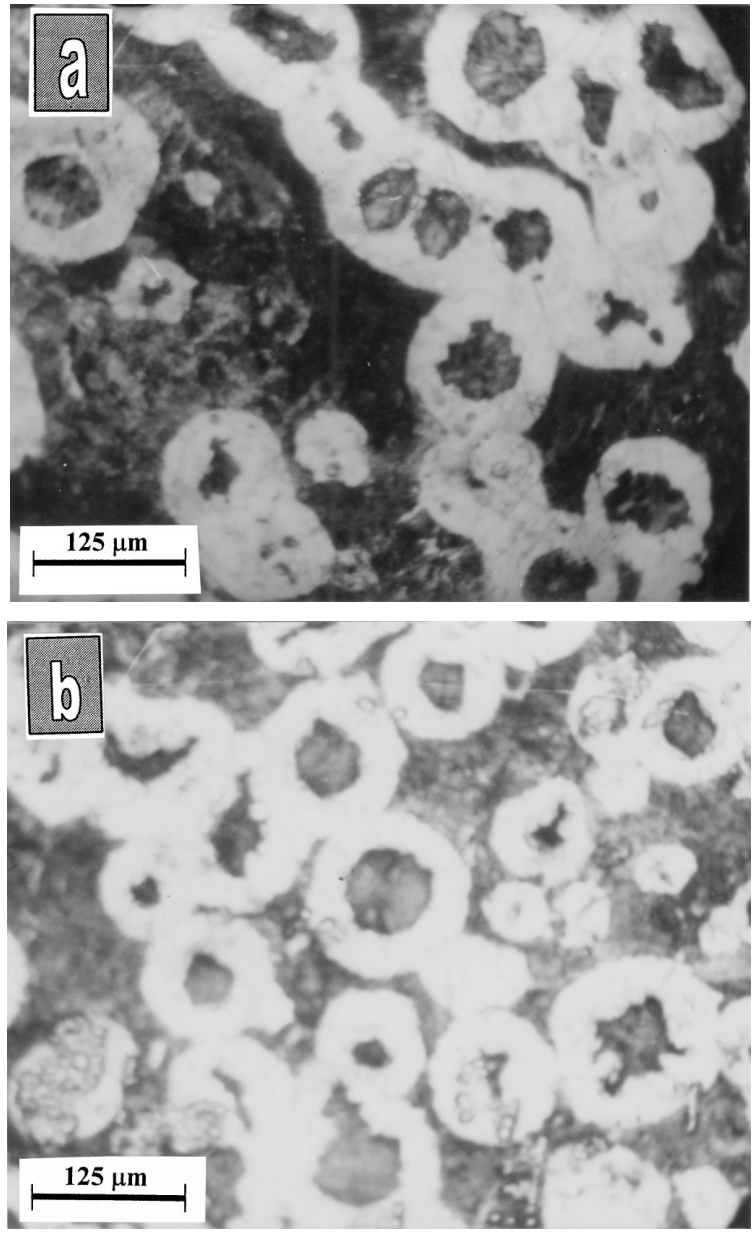

Figure 4 Microstructure of ferritic-pearlitic matrix SG-iron: (a) As-cast; (b) Autenitized at 1193 K and cooled in isolated block, in still-air.

SG-iron with a matrix containing about 75% pearlite. The alloy with a matrix structure of 94.6% pearlite the percentage increase in the UTS is approaching 100% (∼98.24%). The high ductility of ferritic matrix SG-iron (18.9%), displayed in Fig. 6c suggests the ability of this material to allow considerable deformation to occur before fracture takes place. On the other hand, a material with low ductility such as the fully pearlitic SG-iron (5-5.6%), an unforeseen load may cause failure. For clarity, the variation in mechanical properties is calculated as a percentage of the ferritic matrix material. The results are shown in Table III.

3.3. Impact toughness

The fracture energy of SG-irons is influenced significantly by the matrix microstructure. Fracture energy shows a variation similar to that of elongation. As shown in Fig. 7, SG-iron with ferrite matrix exhibits the highest fracture energy (18.4 J). On the other hand,

TABLE III Variation in mechanical properties with pearlite level as a percentage of the ferritic matrix material (−sign means a decrease in the property value)

Pearlite volume fraction (%)	% increase in YS	% increase in UTS	% decrease in elongation	% decrease in impact toughness	% increase in hardness Brinell
41.6	12	26	−50	−37	25
58.5	28	26	−53	−57	37
75.6	84	94	−69	−70	74
94.6	90	98	−74	−76	102

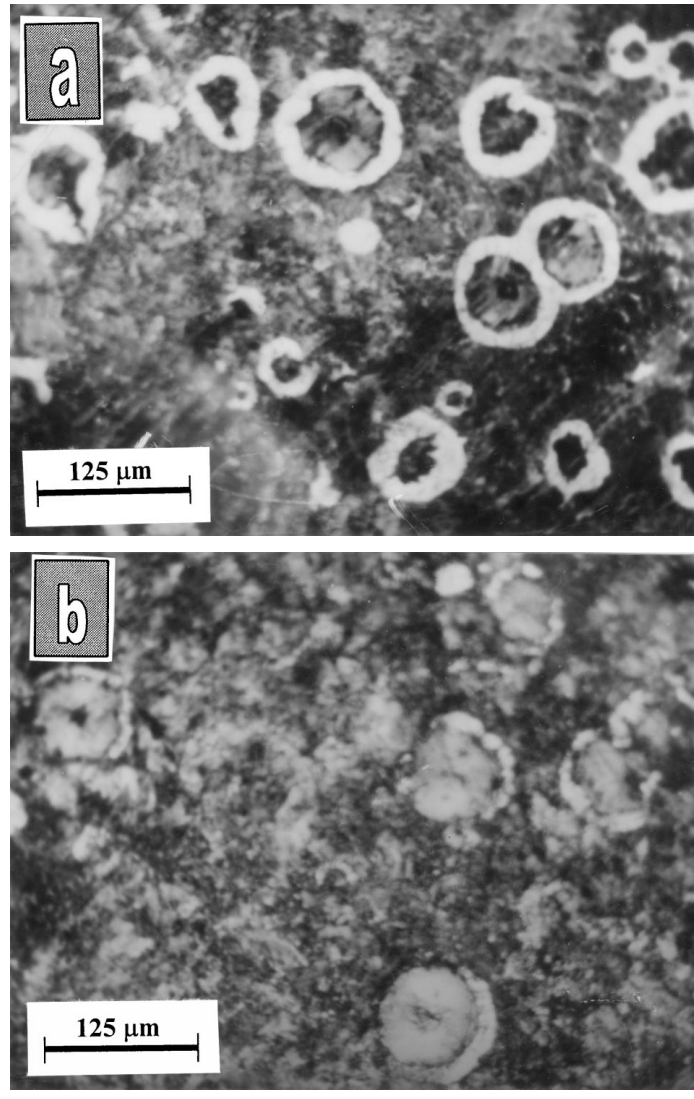

Figure 5 Microstructure of pearlitic matrix SG-iron: (a) Austenitized at 1193 K and cooled in still-air; (b) Austenitized at 1193 K and forced-air cooled.

those with increasing percentage of pearlite, have lower fracture energy. It is worthy to note that when the matrix structure approaches a 100% pearlitic the fracture energy is decreased by an amount of 75.5%. It seems reasonable also to suggest that the difference in the impact toughness among the normalized SG-irons having thinner or no ferrite ring may be due to the capability of a thick ferrite ring to absorb energy through the plastic deformation. This in line with the results of Hwang *et al.* [16] who reported that the "bull's eye" as-cast structure has a higher level of toughness compared with that austenitized at 1103 K for 7.2 ks and then air-cooled. Thus allowing a thick ferrite ring while retaining a pearlitic microstructure may produce a SG-iron, which is able to combine a strength and ductility.

3.4. Hardness

It is well recognized that the hardness of SG-irons depends primarily upon the matrix structure. Since SG-irons used in the present work are produced with a range of pearlite/ferrite matrices (cf. Table II), the effect of the amount of pearlite on the hardness is best demonstrated in these materials. Fig. 8 provides an evidence of the relationships between Brinell hardness and pearlite contents in SG-iron castings in the as cast, fully annealed and normalized conditions respectively. It may be noted that the hardness value increases sharply as the matrix structure approaches a fully pearlitic condition. This can be attributed to the effect of fast cooling rate, which increased the pearlite content and also affected the lamellar spacing, of the pearlitic structure. The latter affects the hardness of the pearlite phase and thus the hardness of the material.

3.5. Fractography

Fig. 9 shows the fracture path in the SG-irons studied. One of the most significant observations noted is the unique behaviour of the graphite nodules and its contribution to the fracture process. Generally, the fracture path propagates around the graphite spheroids leaving them intact in their cavities. This result agrees well with those reported elsewhere [11, 17–19].

In a ferritic-pearlitic matrix structure material (Fig. 9b) the fracture is traveling along a path that connects as many as possible graphite spheroids. It avoids the pearlite structure as much as possible. This observation confirms that of Voigt and Eldoky [17] who reported that even though the strength and toughness of the ferrite and pearlite microconstituents are

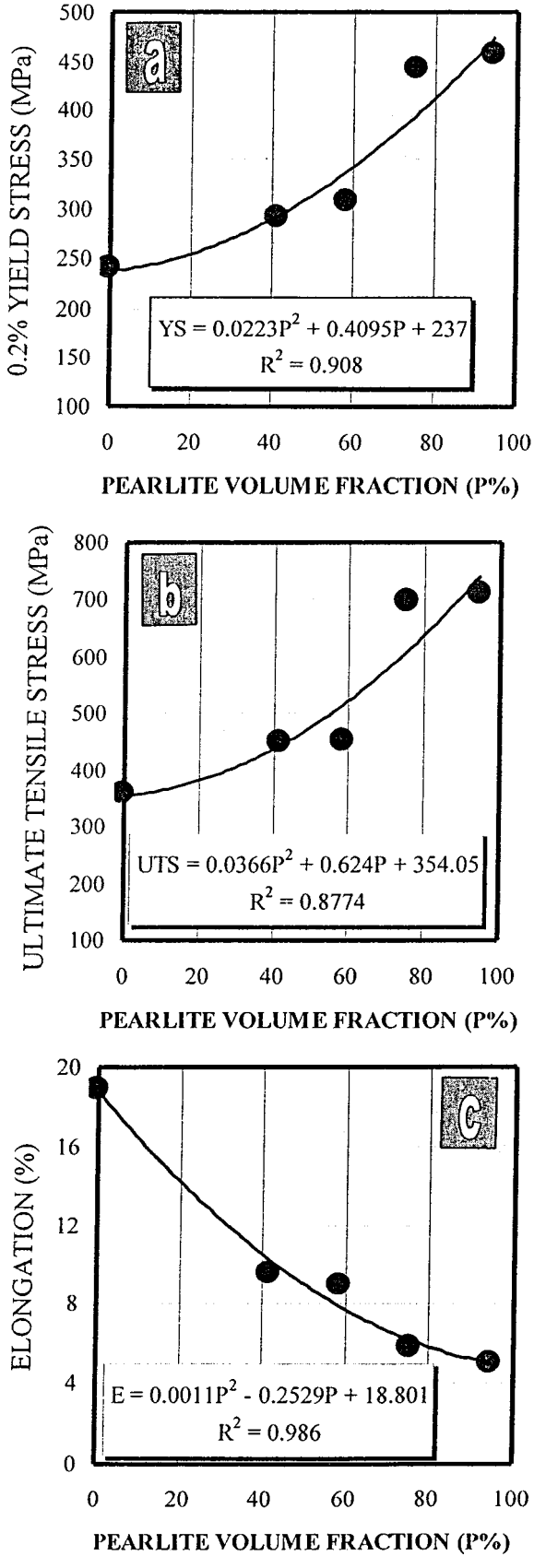

Figure 6 Tensile properties as a function of pearlite content in the matrix: (a) 0.2% yield stress; (b) Ultimate tensile stress; (c) Elongation.

different, a growing crack cannot simply choose to propagate through the low toughness pearlitic regions and avoid the ferrite. This is because the overall fracture path is controlled by initial nodule decohesion and microcracking at the graphite/matrix interface. It is the graphite-nodule distribution that dictates the least energy propagation path and requires the growing crack to travel through the ferrite phase.

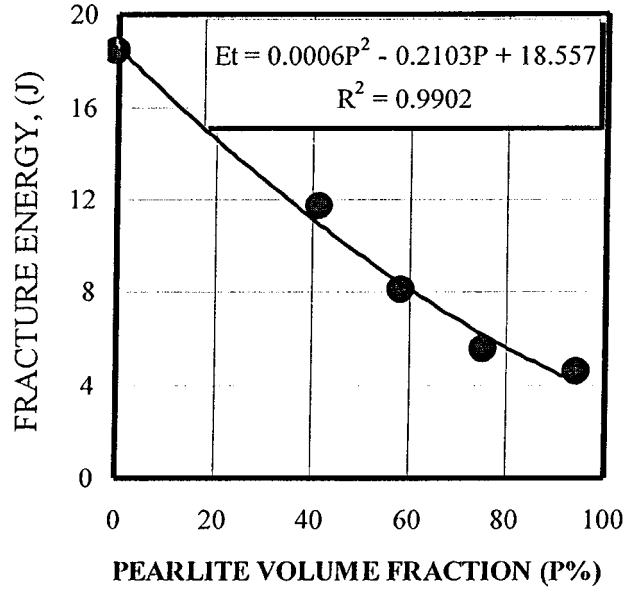

Figure 7 Relationship between the fracture energy and pearlite level in the matrix.

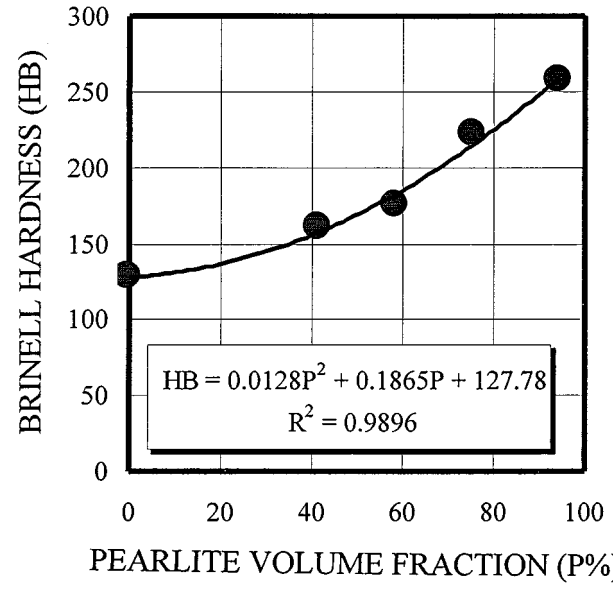

Figure 8 Effect of pearlite content on the hardness of the present SG-iron.

The fracture surface of ferritic SG-iron as revealed by SEM is shown in Fig. 10. Dimple pattern of fracture is found to be the only operative mode of fracture for ferritic SG-iron, as shown in Fig. 10. The features shown in this figure suggest that ferrite deforms to a great extent before the onset of fracture, which starts by the formation and coalescence of voids. This result confirms the high ductility and impact toughness displayed in Figs 6c and 7.

Two different fracture patterns are observed in a ferritic-pearlitic matrix structure. In the vicinity of the graphite nodules, the wider areas of the ferrite phase are deformed considerably. Thus the fracture occurs in a ductile manner. On the other hand, brittle fracture with river pattern in pearlitic areas can be observed. as Fig. 11 indicates.

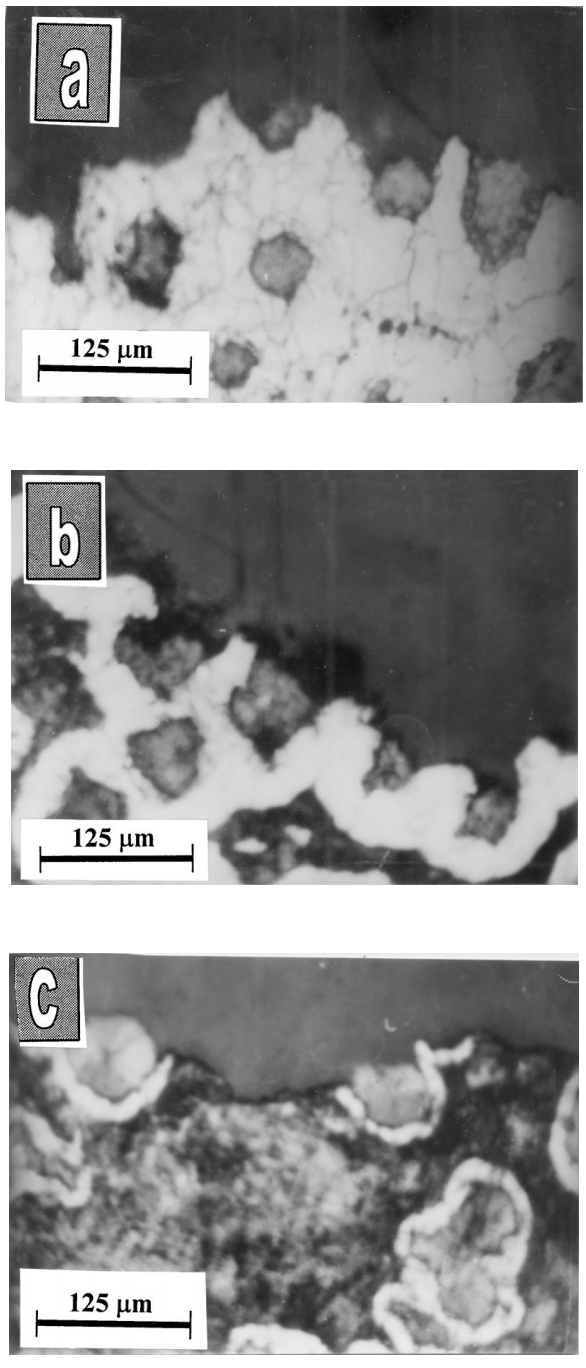

Figure 9 Facture path in the SG-irons studied: (a) Fully ferritic matrix; (b) Ferritic-pearlitic matrix; (c) Pearlitic matrix.

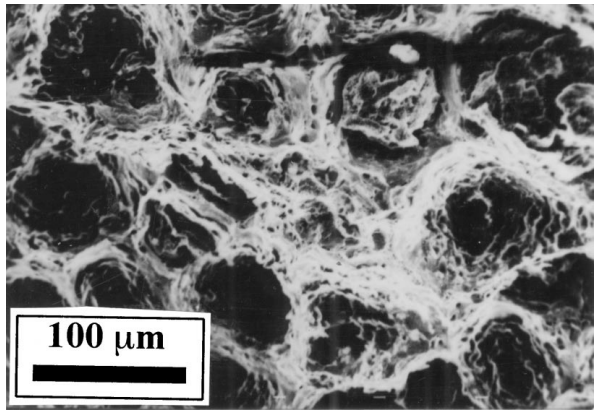

Figure 10 Facture surface of ferritic SG-iron as revealed by SEM.

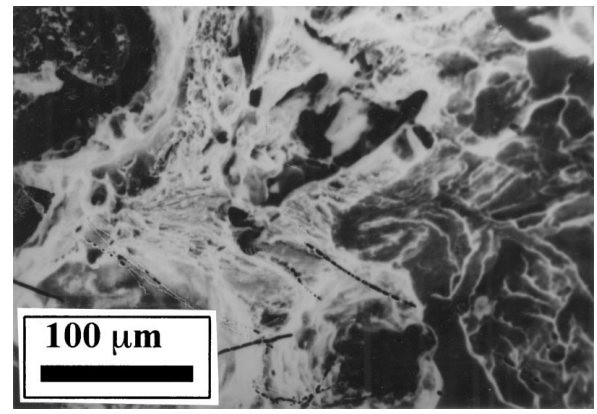

Figure 11 Facture pattern observed in a ferritic-pearlitic matrix structure.

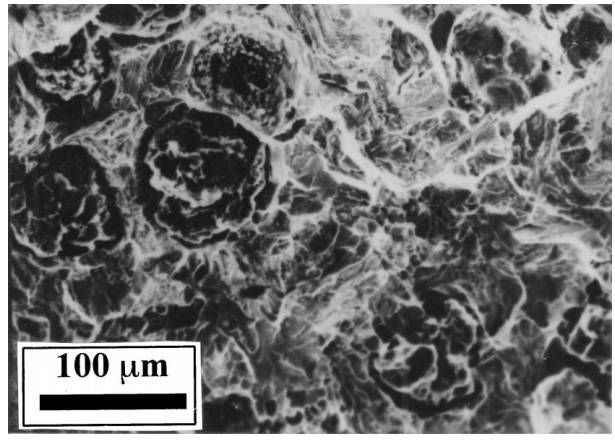

Figure 12 Facture surface of a fully pearlite matrix SG-iron.

Fig. 12 shows the fracture surface of a fully pearlite matrix SG-iron. A complex pattern of fracture reflecting a low energy is delineated in this figure. The fracture surface consists of many cleaved facets. The features of Fig. 12 agree with the low ductility and toughness displayed by this material. Cleavage occurred along the planes of the pearlite lamellae.

4. Conclusions

SG-irons having a variety of matrix structures are prepared. Tensile properties, impact toughness and hardness are measured for the respective cast iron. The effect of the matrix structure on the mechanical properties is discussed. The main conclusions obtained can be summarized as follows:

1. The high ductility of ferritic matrix SG-iron (18.9%), displayed reflects the ability of this material to allow considerable deformation to occur before fracture takes place. On the other hand, in a material with low ductility, such as the fully pearlitic SG-iron (5-5.6%), an unforeseen load may cause failure.

2. Pearlitic grades of SG-iron are a good candidate for applications requiring only high strengths and limited ductility and toughness and are generally not recommended for use in applications requiring impact resistance.

3. The overall fracture path is controlled by initial nodule decohesion and microcracking at the graphite/matrix interface. It is thus the graphite-nodule distributions that dictate the least energy propagation path.

4. Dimple pattern of fracture is found to be the only operative mode of fracture for ferritic SG-iron.

5. Two different fracture patterns are observed in a ferritic-pearlitic matrix structure. In the vicinity of the graphite nodules, the wider areas of the ferrite phase are deformed considerably. Thus the fracture occurs in a ductile manner. On the other hand, brittle fracture with river pattern in pearlitic areas can be observed.

6. A complex pattern of fracture is observed in the fully pearlite matrix SG-iron reflecting the low toughness of this material. The fracture surface consists of many cleaved facets.

References

1. J. GAYET and J. C. MARGERIE, *AFS International Cast Metals Journal* **6**(6) (1981) 47.
2. J. E. BEVAN and W. G. SCHOLZ, *AFS Trans.* **85** (1977) 271.
3. X. P. SHEN, S. J. HARRIS and B. NOBEL, *Materials Science and Technology* **11** (1995) 893.
4. L. GUERIN and M. GAGNE, *Foundryman* **8, 9** (1987) 336.
5. N. FATAHALLA, T. GOMAA, S. BAHI and M. NEGM, *Z. Metallkde* **89**(7) (1998) 507.
6. S. K. YU, C. R. LOPER, JR. and H. H. CORNELL, *AFS Trans.* **94** (1986) 557.
7. D. R. ASKELAND and S. S. GUPTA, *ibid.* **83** (1975) 313.
8. H. BAYATI and R. ELLIOTT, *Materials Science and Technology* **11** (1995) 284.
9. S. C. LIN, T. S. LUI and L. H. CHEN, *AFS Trans.* **105** (1997) 753.
10. P. DIERICKX, C. VERDA, A. REYNAUD and R. FOUGERES, *Scripta Mater.* **34**(2) (1996) 261.
11. J. O. T. ADEWARA and C. R. LOPER, JR, *AFS Trans.* **84** (1976) 513.
12. A. G. FULLER, *ibid.* **85** (1977) 527.
13. ASM, "Metals Handbook- Metallography and Microstructures," Vol. 9, 9th ed. (American Society of Metals, Metal Park, Ohio, USA, 1985).
14. ASM, "Metals Handbook," Vol. 15, 9th ed. (American Society of Metals, Metal Park, Ohio, USA, 1992).
15. S. KARSAY, "Ductile Iron- the Production Practices," 2nd ed. (American Foundrymen's Society for Metals, USA, 1979).
16. J. HWANG, J. DOONG and H. CHEN, *J. Mater. Sci. Letters* **2** (1983) 737.
17. R. C. VOIGT and L. M. ELDOKY, *AFS Trans.* **94** (1986) 637.
18. L. M. ELDOKY and R. C. VOIGT, *ibid.* **93** (1985) 621.
19. J. O. T. ADEWARA and C. R. LOPER, JR, *ibid.* **84** (1976) 527.

Received 7 January
and accepted 2 August 2000